Supplemental Material

A generic dual *d*-band model for interlayer ferromagnetic coupling in transition-metal doped $MnBi_2Te_4$ family of materials

Huisheng Zhang,[*a] Jingjing Zhang,[a] Yaling Zhang,[a] Wenjia Yang,[a] Yingying Wang,[a] Xiaohong Xu,[*a] and Feng Liu[*b]

[a] *College of Physics and Electronic Information & Key Laboratory of Magnetic Molecules and Magnetic Information Materials of Ministry of Education & Research Institute of Materials Science, Shanxi Normal University, Taiyuan, 030031, China*

[b] *Department of Materials Science and Engineering, University of Utah, Salt Lake City, Utah 84112, United States*

Email: hszhang@sxnu.edu.cn, xuxh@sxnu.edu.cn,fliu@eng.utah.edu

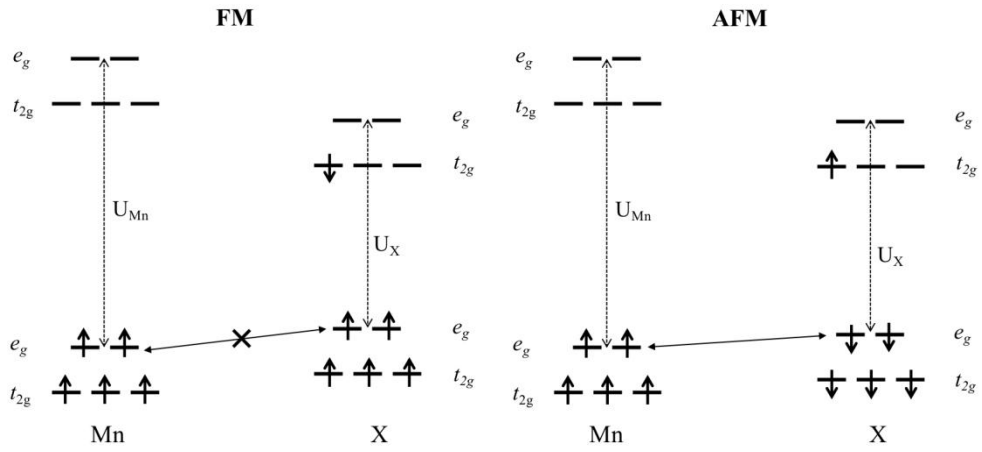

Fig. S1 Schematic diagrams of ferromagnetic (FM) and antiferromagnetic (AFM) coupling in electron-type (namely, Fe, Co, Ni) transition metal doped $MnBi_2Te_4$ (MBT). They illustrate there is no spin channel open for Mn *d*-electron hopping with low energy without spin flipping, so that AFM coupling remains favored.

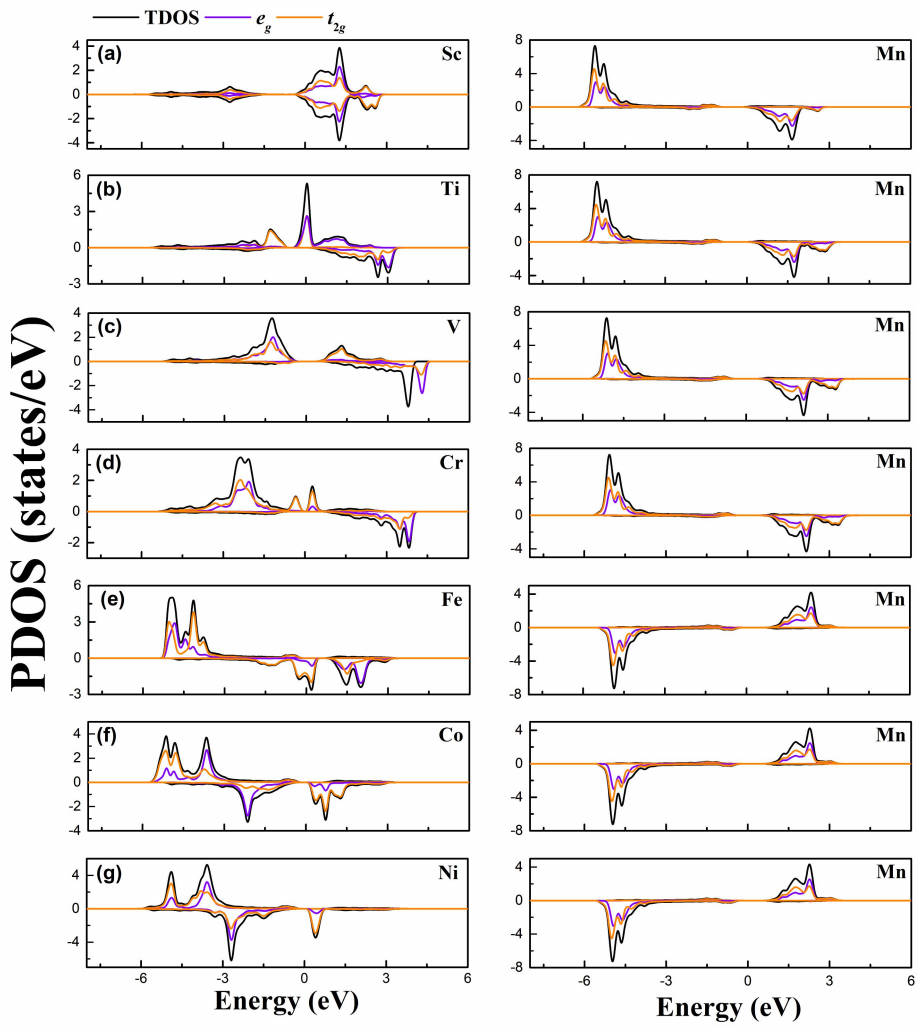

Fig. S2 Calculated partial density of states (PDOS) of Sc (a), Ti (b), V (c), Cr (d), Fe (e), Co, (f) and Ni (g)-doped $MnBi_2Te_4$. For comparison, the PDOS of Mn is also given for each system. Fermi levels are set to zero.

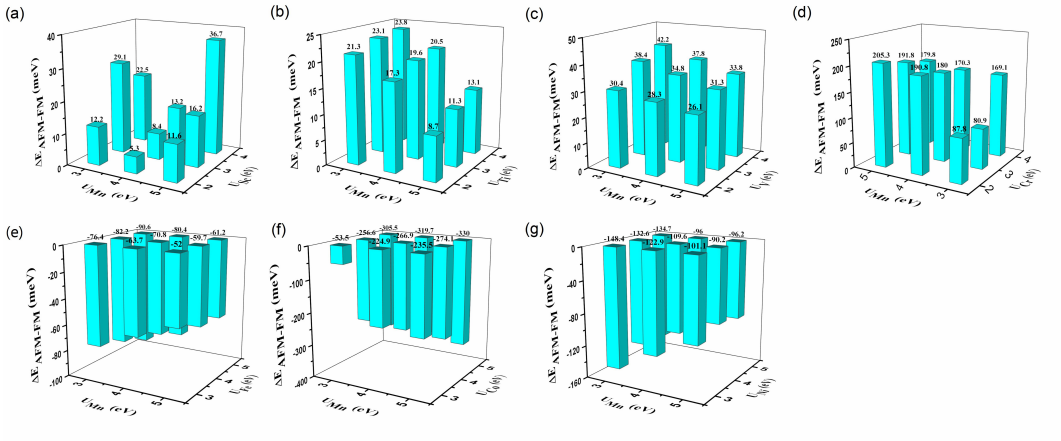

Fig. S3 Calculated energy difference $\Delta E_{\text{AFM-FM}}$ of the Sc (a), Ti (b), V (c), Cr (d), Fe (e), Co, (f) and Ni (g)-doped $Mn_2Bi_2Te_5$ monolayers with different effective U parameters.

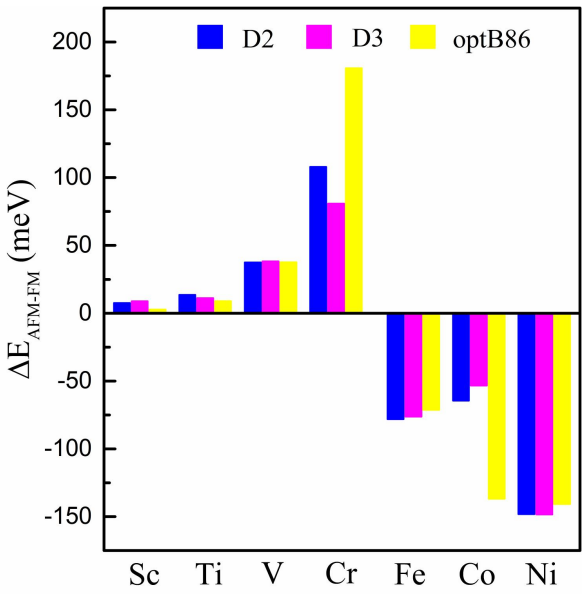

Fig. S4 Calculated energy difference $\Delta E_{\text{AFM-FM}}$ of the X-doped (X = Sc, Ti, V, Cr, Fe, Co, or Ni) $Mn_2Bi_2Te_5$ monolayers by using vdW correction of DFT-D2, DFT-D3, and opbB86, respectively.

	Magnetic configurations			
	AFM			FM
	↑ ↓ ↑ ↓	↑ ↓ ↓ ↑	↑ ↑ ↓ ↓	↑ ↑ ↑ ↑
$E_{MnScBi_2Te_5}$ (eV)	-83.911	-83.910	-83.914	-83.916
$E_{MnTiBi_2Te_5}$ (eV)	-84.406	-84.407	-84.423	-84.429
$E_{MnVBi_2Te_5}$ (eV)	-85.721	-85.723	-85.791	-85.799
$E_{MnCrBi_2Te_5}$ (eV)	-86.600	-86.599	-86.940	-86.951

Fig. S5 Total energies of $MnScBi_2Te_5$, $MnTiBi_2Te_5$, $MnVBi_2Te_5$, and $MnCrBi_2Te_5$ bilayers for three types of antiferromagnetic (AFM) and one type ferromagnetic (FM) orders.

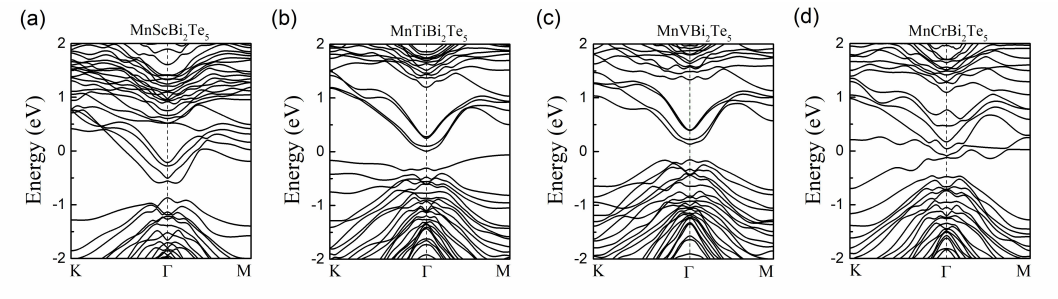

Fig. S6 The electronic band structures of $MnScBi_2Te_5$ (a), $MnTiBi_2Te_5$ (b), $MnVBi_2Te_5$ (c), and $MnCrBi_2Te_5$ (d) including spin-orbit coupling, respectively.

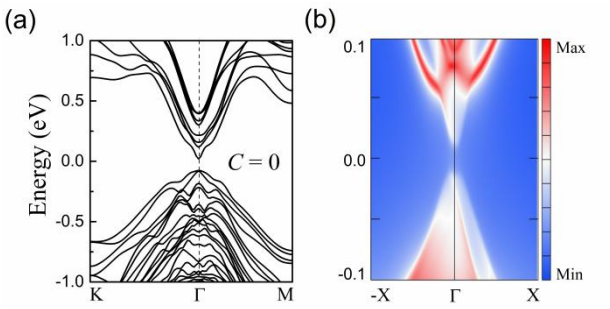

Fig. S7 (a) The electronic band structures of $MnVBi_2Te_5$ bilayer, where the calculated Chern number *C* is 0. (b) The corresponding bands showing no edge state.

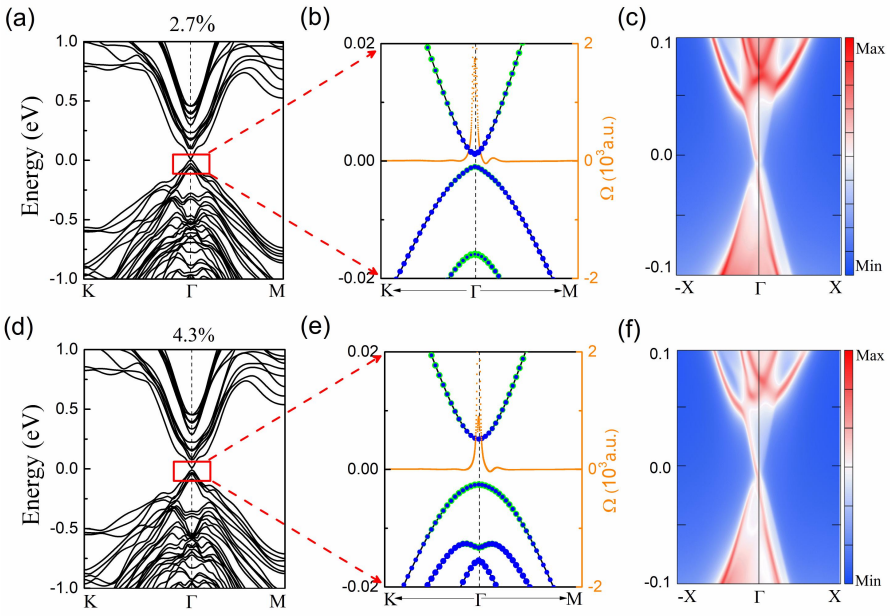

Fig. S8 (a) Electronic band structures of $MnVBi_2Te_5$ trilayer by applying 2.7% biaxial tensile strain. (b) Magnified bands near Fermi level in (a), where projected bands of Bi-p_z and Te-p_z orbitals are also given. (c) The corresponding edge states. (d)-(f) The same as (a)-(c) for $MnVBi_2Te_5$ trilayer with 4.3% biaxial tensile strain. Fermi levels are set to zero.

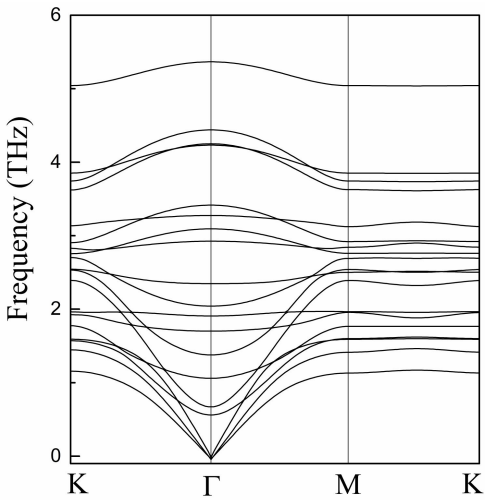

Fig. S9 Calculated phonon spectra of $MnVBi_2Te_5$ monolayer.

(a)

Structual configurations	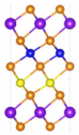 (I)	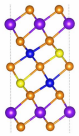 (II)	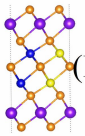 (III)
E_{FM} (eV) ↑↑↓↓	-85.425206	-85.409106	-85.487828
E_{AFM} (eV)↑↑↓↓	-85.388309	-85.479983	-85.406927

(b)

Structual configurations	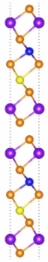	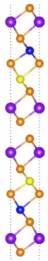	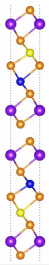
E_{FM} (eV) ↑↑↑↑	-85.799402	-85.796374	-85.790626
E_{AFM} (eV) ↑↑↓↓	-85.798253	-85.796558	-85.792183
E_{AFM} (eV) ↑↓↑↓	-85.721508	-85.720240	-85.725749
E_{AFM} (eV) ↑↓↓↑	-85.723198	-85.719410	-85.723668

Fig. S10 (a) Total energies of FM and AFM $MnVBi_2Te_5$ monolayer in a 2 × 1 ×1 supercell. (b) The same as (a) for $MnVBi_2Te_5$ bilayer. The black arrows denote the directions of magnetic moments of V or Mn.

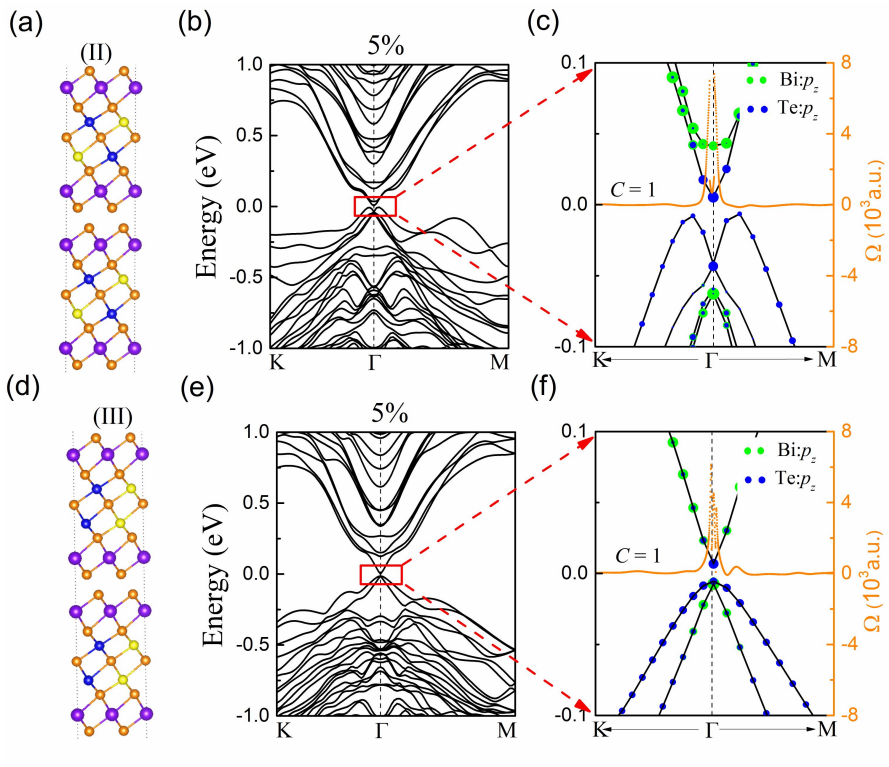

Fig. S11 (a) Structural configuration (II) of $MnVBi_2Te_5$ bilayer in Fig. S10. (b) Corresponding electronic band structure by applying 5.0% biaxial tensile strain. (c) Magnified bands near Fermi level in (b), where projected bands of Bi-p_z and Te-p_z orbitals are also given. (d)-(f) The same as (a)-(c) for structural configuration (III) of $MnVBi_2Te_5$ bilayer in Fig. S10. Fermi levels are set to zero.

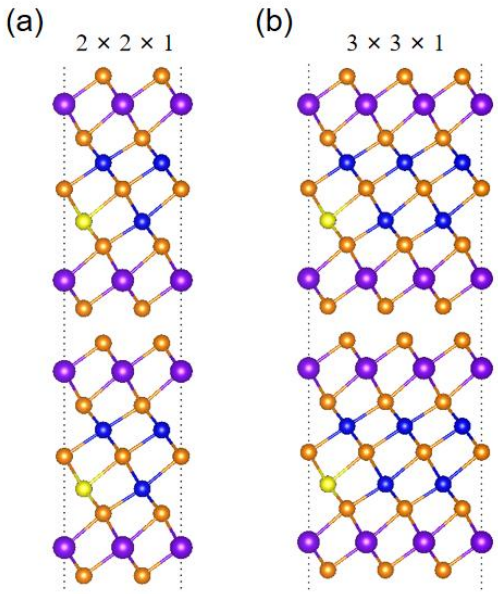

Fig. S12 The crystal structures of V-doped M_2BT with the 25% (a) and 11.1% (b) doping concentration, respectively.